Supporting Information

Sharifnia et al. 10.1073/pnas.1412228112

SI Materials and Methods

Cell Culture and Reagents. The *EGFR*-mutant NSCLC cell lines PC9 (del E746_A750), HCC827 (del E746_A750), HCC2279 (del E746_A750), H3255 (L858R), and HCC2935 (del E746_T751, S752I) have been described previously (1–7). The *EML4-ALK* NSCLC cell line H3122 (*EML4-ALK* variant 1 E13;A20) has been described previously (8) and was obtained from the National Cancer Institute. Cells were maintained in RPMI (CellGro) supplemented with 10% FBS (Gemini Bio Products). Erlotinib, dasatinib, and lestaurtinib were purchased from LC Laboratories. NVP-BGJ398, XL880, NVP-BEZ235, AZD6244, TAE684, and AZ628 were purchased from Selleck Chemicals. BMS-509744 was purchased from EMD Millipore. Lapatinib was purified from patient-discarded tablets by James Bradner, Dana-Farber Cancer Institute, Boston. Cisplatin was obtained from the Dana–Farber Cancer Institute Pharmacy and was manufactured by APP Pharmaceuticals.

Kinase ORF Screen. Screening was performed using a kinase ORF library of 589 ORFs encoding 584 genes (CCSB/Broad Institute Kinase ORF Collection) (9, 10), along with the positive and negative controls described in the main text and displayed in Fig. 1. PC9 cells were seeded overnight in 384-well microtiter plates at a density of 400 cells per well. The following day, cells were incubated with lentivirus corresponding to the kinase ORF library and controls in the presence of 4 μg/mL polybrene, spin-infected at 1,126 × *g* for 30 min at 30 °C, then incubated at 37 °C for an additional 4.5 h before replacing media with standard growth media. At 24 h postinfection, standard growth media (six replicates) or media containing 2 μg/mL blasticidin (one replicate) was spiked into wells. At 72 h postinfection, media was replaced with media containing 3 μM erlotinib (two replicates), 300 nM erlotinib (two replicates), DMSO (two replicates), or DMSO + 2 μg/mL blasticidin (one blasticidin-treated replicate). Cell viability was assayed 3 d after the addition of erlotinib/DMSO using the CellTiter-Glo reagent (Promega).

Identification of Candidate EGFR Bypass Genes. Raw luminescence values representing cell viability were averaged between replicates, following exclusion of wells failing detection or other quality control criteria (0.5% of wells). For each of the two drug dose screening arms, for a given ORF or control, viability under erlotinib treatment was normalized to that under DMSO treatment. Candidate EGFR bypass genes were defined as those having relative viability values of at least 39% in 300 nM erlotinib and at least 31% in 3 μM erlotinib. Luminescence values corresponding to DMSO + blasticidin-treated cells were compared with those of (unselected) DMSO-treated cells to assess each ORF's infection efficiency.

Screen Validation and Drug Sensitivity Assays. PC9, HCC827, HCC2935, HCC2279, H3255, and H3122 cells were seeded overnight in 384-well microtiter plates at a density of 400, 500, 1,200, 800, 1,100, and 1,000 cells per well, respectively. The following day, cells were incubated with lentivirus (virus production methods described below) corresponding to candidate EGFR bypass ORFs as well as controls in the presence of 4 μg/mL polybrene, spin-infected at 1,126 × *g* for 30 min at 30 °C, then incubated at 37 °C for an additional 4.5 h before replacing media with standard growth media. At 24 h postinfection, additional standard growth media was spiked into wells. At 72 h postinfection, media was replaced with media containing inhibitor(s) at their final concentrations or DMSO (1:1,000 dilution). For dose–response curves, inhibitor(s) were tested at each of the following concentrations: 10, 1, 0.1, 0.01, 0.001, and 0.0001 μM. Cell viability was assayed 3 d after the addition of inhibitor(s) or DMSO using CellTiter-Glo (Promega). Drug-treated cells were normalized to DMSO-treated cells to calculate relative percent viability. Relative percent viability values and dose–response curves were plotted using GraphPad Prism software (GraphPad); AUC values were generated using GraphPad Prism software and displayed using GENE-E software. Absolute IC_{50} values were calculated using GraphPad Prism software.

Drug sensitivity assays with cisplatin were modified from above as follows: PC9 cells were seeded at a density of 200 cells per well, cells were treated with inhibitor/DMSO at 48 h postinfection, and the inhibitor was tested at concentrations of 50, 10, 5, 1, 0.1, and 0.01 μM.

The cluster analysis displayed in Fig. 2*B* was performed as follows: relative percent viability values generated from cells treated with 1 μM (PC9) or 3 μM erlotinib (HCC2279, HCC2935, H3255, HCC827) were used to perform a one-tailed, unpaired *t* test (bypass ORFs vs. *LACZ*). We performed *t* tests for all bypass ORFs whose effects led to any increase in mean relative percent viability compared with *LACZ*; otherwise, the effect of the bypass ORF was assigned a value of zero (no increase). Significance values were converted into an ordinal scale of resistance values according to the following thresholds: 0, no increase or insignificant increase ($P \geq 0.05$) in relative percent viability compared with LACZ-transduced cells; +1, significant increase in relative percent viability ($0.01 < P < 0.05$); +2, very significant increase in relative percent viability ($0.001 < P < 0.01$); +3, extremely significant increase in relative percent viability ($0.0001 < P < 0.001$); +4, extremely significant increase in relative percent viability ($P < 0.0001$). ORF and cell line ordinal resistance profiles were each grouped using a Euclidean distance metric and complete linkage hierarchical clustering. Cluster analysis and visualization was performed using R (www.r-project.org).

The heat map in Fig. S2*E* was constructed by considering the *P* values (and "no increase" criteria) calculated above, and among ORFs with significant resistance-inducing effects, by using the fold-change in viability induced by a given ORF under erlotinib treatment relative to *LACZ*. Visualization was performed using R.

Virus Production. Lentivirus was produced by transfection of 293T packaging cells with plasmids corresponding to pLX-Blast-V5-ORF, Δ8.9 (*gag, pol*), and VSV-G; and FuGene6 transfection reagent (Roche) as described previously (9).

Viral Transduction and Culture of ORF-Expressing Cells for Protein Analysis. PC9 and H3255 cells were seeded in six-well plates at a density of 54,000 and 120,000 cells per well, respectively. The next day, cells were incubated with lentivirus in the presence of 4 μg/mL polybrene for 6–7 h, after which media was replaced with standard growth media. At 24 h postinfection, media was replaced with selective media containing 1–1.3 μg/mL (PC9) or 8 μg/mL (H3255) blasticidin, and blasticidin-containing media was replenished after another 72 h. Where noted, at 6 d postinfection, cells were treated with media containing 0.5% FBS overnight. The following day, cells were treated with inhibitor(s) or DMSO at their final concentrations in media containing 0.5% FBS for 6 h, then harvested for immunoblotting. Otherwise, cells were harvested for immunoblotting 6 d postinfection (in these cases, PC9 cell seeding density was 36,000 cells per well).

Immunoblotting. Cell pellets were resuspended in lysis buffer [50 mM Tris (pH 7.4), 2.5 mM EDTA (pH 8), 150 mM NaCl, 1% Triton X-100, 0.25% IGEPAL CA-630] supplemented with protease inhibitors (Roche) and Phosphatase Inhibitor Mixtures I and II (Calbiochem), incubated on ice for at least 2 min, then centrifuged for 2 min at 15,700 × *g*. The protein concentrations of supernatants were determined using a BCA Protein Assay Kit (Pierce) and normalized. Lysates were reduced and denatured, then separated using Tris-Glycine gels (Novex) and transferred to iBlot Transfer Stack nitrocellulose membranes (Novex). Membranes were incubated with primary antibodies overnight at 4 °C. Antibodies against phospho-EGFR (Y1068; 1:1,000) and V5 (1:5,000) were purchased from Invitrogen. The antibody recognizing total EGFR (1:1,000) was purchased from BD Biosciences. Antibodies against total AKT (1:1,000), phospho-AKT (S473 and T308), total AXL (1:1,000), phospho-AXL (Y702; 1:500), β-actin (1:10,000), cofilin (1:10,000), phospho-EGFR (Y845; 1:500), total ERBB2 (1:1,000), phospho-ERBB2 (Y1221/1222; 1:500), total ERK1/2 (1:750), phospho-ERK1/2 (T202/Y204; 1:500), total FGFR1 (1:1,000), total FGFR2 (1:1,000), phospho-FGFR (Y653/654; 1:500), total LCK (1:1,000), total LYN (1:1,000), total NTRK1 (1:1,000), phospho-NTRK1 (Y674/675; 1:500), total RAF1 (1:1,000), phospho-RAF1 (S338; 1:500), total SRC (1:1,000), and phospho-SRC family (Y416; 1:500) were purchased from Cell Signaling Technology. The phospho-SRC family antibody (Y416) may cross-react with other Src family members, including LCK and LYN. Phospho-AKT immunoblotting was performed with the S473-directed antibody (1:750) unless otherwise indicated. Phospho-EGFR immunoblotting was performed with the Y1068-directed antibody unless otherwise indicated. Incubation with IRDye secondary antibodies (1:10,000; LI-COR Biosciences) and subsequent detection (Odyssey Imaging System, LI-COR Biosciences) were performed according to manufacturer recommendations.

CCLE NSCLC Gene Expression Data. Microarray gene expression data for 186 non-small cell lung cancer cell lines were obtained from the Broad–Novartis Cancer Cell Line Encyclopedia (www.broadinstitute.org/ccle/). The 2,000 most-varying genes demonstrating >6 $\log_2$ robust multiarray average (RMA) units of mean expression across these data were used to group the cell lines using complete linkage hierarchical clustering and a Euclidean distance metric. Cluster analysis and visualization was performed using R.

Gene Expression Profiling and LINCS Analysis. ORFs selected for profiling included 18 validated bypass-promoting ORFs; 19 kinase ORFs unable to confer EGFR bypass in the primary ORF screen (as measured by a *z*-score less than 0.2 under both drug doses); as well as controls. PC9 cells were seeded overnight in 384-well microtiter plates at a density of 400 cells per well. The following day, cells were incubated with lentivirus corresponding to ORFs in the presence of 4 μg/mL polybrene, spin-infected at 1,126 × *g* for 30 min at 30 °C, then incubated at 37 °C for an additional 4.5 h before replacing media with standard growth media. At 24 h postinfection, additional standard growth media was spiked into wells. At 72 h postinfection, media was replaced with media containing 300 nM erlotinib. After 24 h of drug treatment, media was aspirated and replaced with TCL Buffer (Qiagen) for cell lysis. Plates were incubated at 25 °C for 25 min, then stored at −80 °C until gene expression-profiling steps.

Gene expression profiles consisted of 978 transcripts that were selected by the LINCS program (www.lincscloud.org) to represent an unbiased reduced representation of the transcriptome and measured using a Luminex bead-based system (11). Each ORF was assayed and profiled in quadruplicate, and all expression data were quantile-normalized. To quantify the magnitude of differential expression in our data, we computed robust *z*-scores for each gene in each sample according to

$$z_i = \frac{X_i - \text{median}(Y)}{\text{MAD}(Y) \times 1.4826},$$

where X_i is the scaled expression value of the sample of interest, Y is the vector of observed control expression values for the gene of interest, and MAD is the mean absolute deviation.

After computing a robust *z*-score vector for each replicate, we combined the robust *z*-scored replicate vectors into a single representative vector that we refer to as a signature. Unsupervised hierarchical clustering using the Spearman correlation metric was performed on signatures generated from PC9 cells expressing 18 EGFR bypass-inducing genes, 19 kinases unable to induce EGFR bypass, and controls. Hierarchical clustering revealed a tight cluster comprised of 12 bypass-promoting genes and the two *EGFR* double-mutant positive controls. For the LINCS ORF query, signatures from each of the 12 bypass-promoting genes were used to independently query 2,537 ORF signatures in the LINCS dataset. Each LINCS ORF–bypass ORF query pair was assigned a connectivity score (12) computed using the weighted Kolmogorov–Smirnov statistic (13). All LINCS ORFs in the dataset were rank ordered by their connectivity scores to a given bypass ORF query. The top ∼3% positively correlated LINCS ORFs are listed per bypass ORF query in Fig. 4*B*.

For the LINCS compound query, signatures from each of the 12 bypass-promoting genes were used to independently query 34,148 compound signatures in the LINCS dataset. Each compound–ORF query pair was assigned a connectivity score as described above. All compounds in the dataset were rank ordered by their connectivity scores to a given ORF query. To identify compounds that were consistently correlated/anti-correlated to the query ORFs, we computed every compound's median normalized rank across all 12 ORFs. The resultant ranks are displayed in Fig. 5*A*.

Caspase-3/7 Activation Assay. PC9 cells were seeded overnight in 384-well microtiter plates at a density of 400 cells per well. The following day, cells were incubated with lentivirus corresponding to ORFs in the presence of 4 μg/mL polybrene, spin-infected at 1,126 × *g* for 30 min at 30 °C, then incubated at 37 °C for an additional 4.5 h before replacing media with standard growth media. At 24 h postinfection, additional standard growth media was spiked into wells. At 72 h postinfection, media was replaced with media containing DMSO, erlotinib, the relevant kinase inhibitor, or their combinations, at their final concentrations. Caspase-3/7 activity was assayed 26 h after the addition of inhibitor(s) or DMSO with the Caspase-Glo 3/7 reagent (Promega). Luminescence values corresponding to drug-treated cells were normalized to those of DMSO-treated cells to calculate relative caspase-3/7 activation.

In-Cell Western for Protein Expression. PC9 cells were seeded overnight in black, clear-bottom 384-well microtiter plates at a density of 1,300 cells per well. The following day, cells were incubated with lentivirus corresponding to 77 randomly selected ORFs from the CCSB/Broad kinase ORF library in the presence of 4 μg/mL polybrene, spin-infected at 1,126 × *g* for 30 min at 30 °C, then incubated at 37 °C for an additional 4.5 h before replacing media with standard growth media. At 24 h postinfection, standard growth media was spiked into wells. At 72 h postinfection, cells were fixed with 4% formaldehyde and 0.1% Triton X-100 in PBS for 30 min. Fixative was removed, and cells were washed with PBS, then blocked for 30 min at room temperature. Cells were incubated with primary antibody

(1:5,000 dilution of anti-V5; Invitrogen) overnight at 4 °C. Cells were washed three times with 0.1% Tween-20 in H_20, then incubated with a mix of secondary antibody and cell stains [1:800 dilution of IRDye 800CW goat anti-mouse (LI-COR); 1:10,000 dilution of DRAQ5 (Cell Signaling); and 1:1,000 dilution of Sapphire700 (LI-COR)] for 1 h at RT. Cells were washed three times with 0.1% Tween-20 in H_20, and once with PBS, before scanning using the LI-COR Odyssey. Quantification of fluorescence was performed using LI-COR Image Studio software.

Statistical Tests. One-tailed, unpaired *t* tests were calculated using GraphPad Prism software. *P* values less than 0.05 were considered significant.

1. Paez JG, et al. (2004) EGFR mutations in lung cancer: Correlation with clinical response to gefitinib therapy. *Science* 304(5676):1497–1500.
2. Sos ML, et al. (2009) Predicting drug susceptibility of non-small cell lung cancers based on genetic lesions. *J Clin Invest* 119(6):1727–1740.
3. Engelman JA, et al. (2006) Allelic dilution obscures detection of a biologically significant resistance mutation in EGFR-amplified lung cancer. *J Clin Invest* 116(10): 2695–2706.
4. Ono M, et al. (2004) Sensitivity to gefitinib (Iressa, ZD1839) in non-small cell lung cancer cell lines correlates with dependence on the epidermal growth factor (EGF) receptor/extracellular signal-regulated kinase 1/2 and EGF receptor/Akt pathway for proliferation. *Mol Cancer Ther* 3(4):465–472.
5. Ercan D, et al. (2010) Amplification of EGFR T790M causes resistance to an irreversible EGFR inhibitor. *Oncogene* 29(16):2346–2356.
6. Koivunen JP, et al. (2008) Mutations in the LKB1 tumour suppressor are frequently detected in tumours from Caucasian but not Asian lung cancer patients. *Br J Cancer* 99(2):245–252.
7. Lu Y, Liang K, Li X, Fan Z (2007) Responses of cancer cells with wild-type or tyrosine kinase domain-mutated epidermal growth factor receptor (EGFR) to EGFR-targeted therapy are linked to downregulation of hypoxia-inducible factor-1alpha. *Mol Cancer* 6:63.
8. Koivunen JP, et al. (2008) EML4-ALK fusion gene and efficacy of an ALK kinase inhibitor in lung cancer. *Clin Cancer Res* 14(13):4275–4283.
9. Johannessen CM, et al. (2010) COT drives resistance to RAF inhibition through MAP kinase pathway reactivation. *Nature* 468(7326):968–972.
10. Yang X, et al. (2011) A public genome-scale lentiviral expression library of human ORFs. *Nat Methods* 8(8):659–661.
11. Peck D, et al. (2006) A method for high-throughput gene expression signature analysis. *Genome Biol* 7(7):R61.
12. Lamb J, et al. (2006) The Connectivity Map: Using gene-expression signatures to connect small molecules, genes, and disease. *Science* 313(5795):1929–1935.
13. Subramanian A, et al. (2005) Gene set enrichment analysis: A knowledge-based approach for interpreting genome-wide expression profiles. *Proc Natl Acad Sci USA* 102(43):15545–15550.

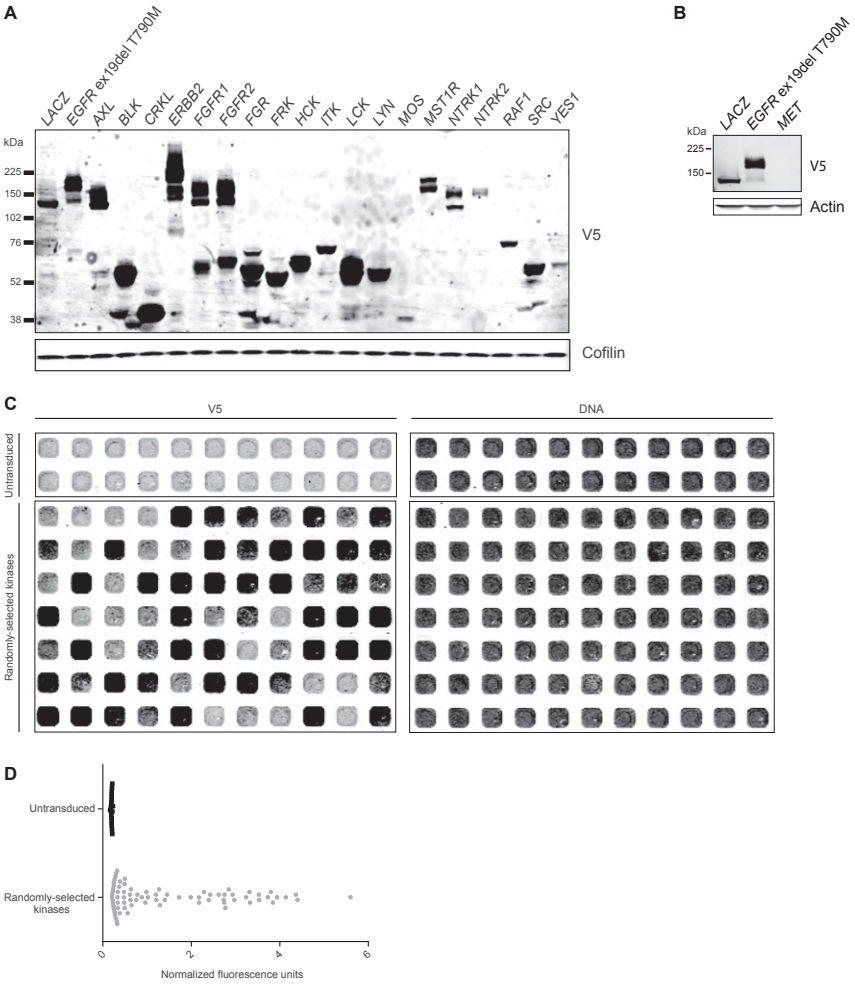

Fig. S1. Protein expression of ectopically expressed ORFs. (*A*) Immunoblot analysis of PC9 cells overexpressing candidate bypass-mediating ORFs and controls following treatment with DMSO for 6 h. Cells were incubated with 0.5% serum media 18 h before and during DMSO treatment. Total cell lysates were immunoblotted for V5-tagged, ectopic protein expression using a V5-directed antibody. (*B*) Immunoblot analysis of PC9 cells transduced with *MET* and control genes. Total cell lysates were immunoblotted for V5-tagged, ectopic protein expression using a V5-directed antibody. (*C*) In-cell western of PC9 cells transduced with 77 randomly selected kinase ORFs. Ectopic, V5-epitope-tagged protein levels (*Left*) and total cellular DNA levels (*Right*) were measured for transduced cells and untransduced controls. *Left* and *Right* represent the same wells on a single plate of cells. (*D*) Quantification of fluorescent signal displayed in *C*. Data are expressed as V5-associated signal relative to that of total DNA. Greater than 93% of randomly selected kinases induce signal above two SDs from the mean of negative controls.

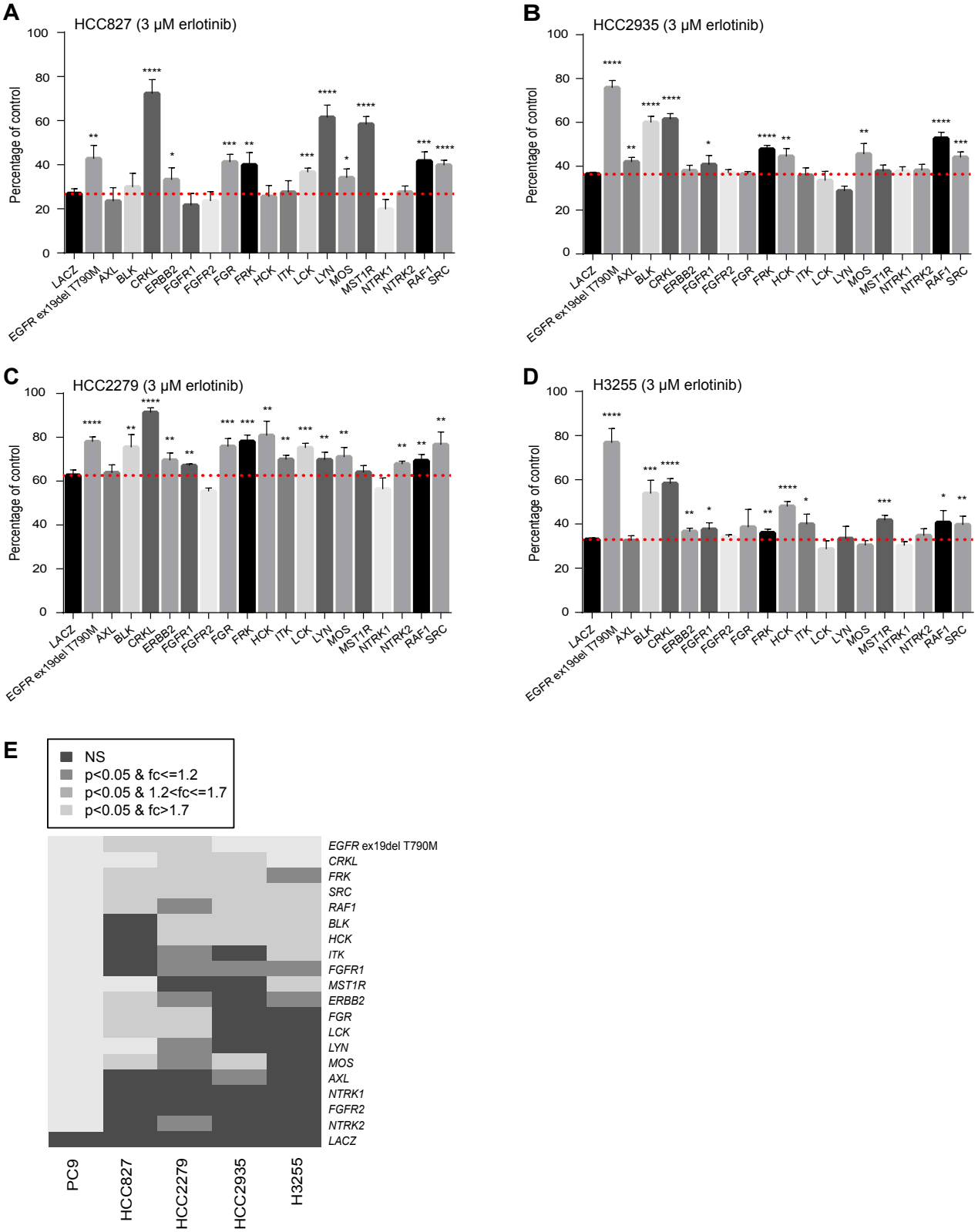

Fig. S2. Validation of candidate EGFR bypass genes in additional *EGFR*-mutant cell lines. (*A*) HCC827, (*B*) HCC2935, (*C*) HCC2279, and (*D*) H3255 cells were transduced with the 18 EGFR bypass genes validated in PC9 cells and controls, treated with 3 μM erlotinib or vehicle, then assayed for cell viability after 72 h using CellTiter-Glo. Data are expressed as percent viability relative to vehicle-treated cells and represent the mean ± SD of four replicates. The mean percent viability of *LACZ*-expressing cells under erlotinib treatment is denoted with a dashed red line. One-tailed, unpaired *t* tests were performed for bypass ORFs whose mean percent viability exceeded this dashed line. *$P < 0.05$; **$0.001 < P < 0.01$; ***$0.0001 < P < 0.001$; ****$P < 0.0001$ (indicated ORF vs. *LACZ*). (*E*) Heat map summarizing effects of bypass ORFs validated in Fig. 2*A* across five *EGFR*-mutant cell line models. Black tiles represent nonsignificant (NS) ORF-induced

Legend continued on following page

erlotinib resistance ($P \geq 0.05$ or no increase in viability relative to *LACZ*); grayscale represents increasing fold-change (fc) in viability (relative to *LACZ* controls) among ORFs with significant effects ($P < 0.05$). Data were generated from cells treated with 1 μM (PC9) or 3 μM erlotinib (HCC2279, HCC2935, H3255, HCC827).

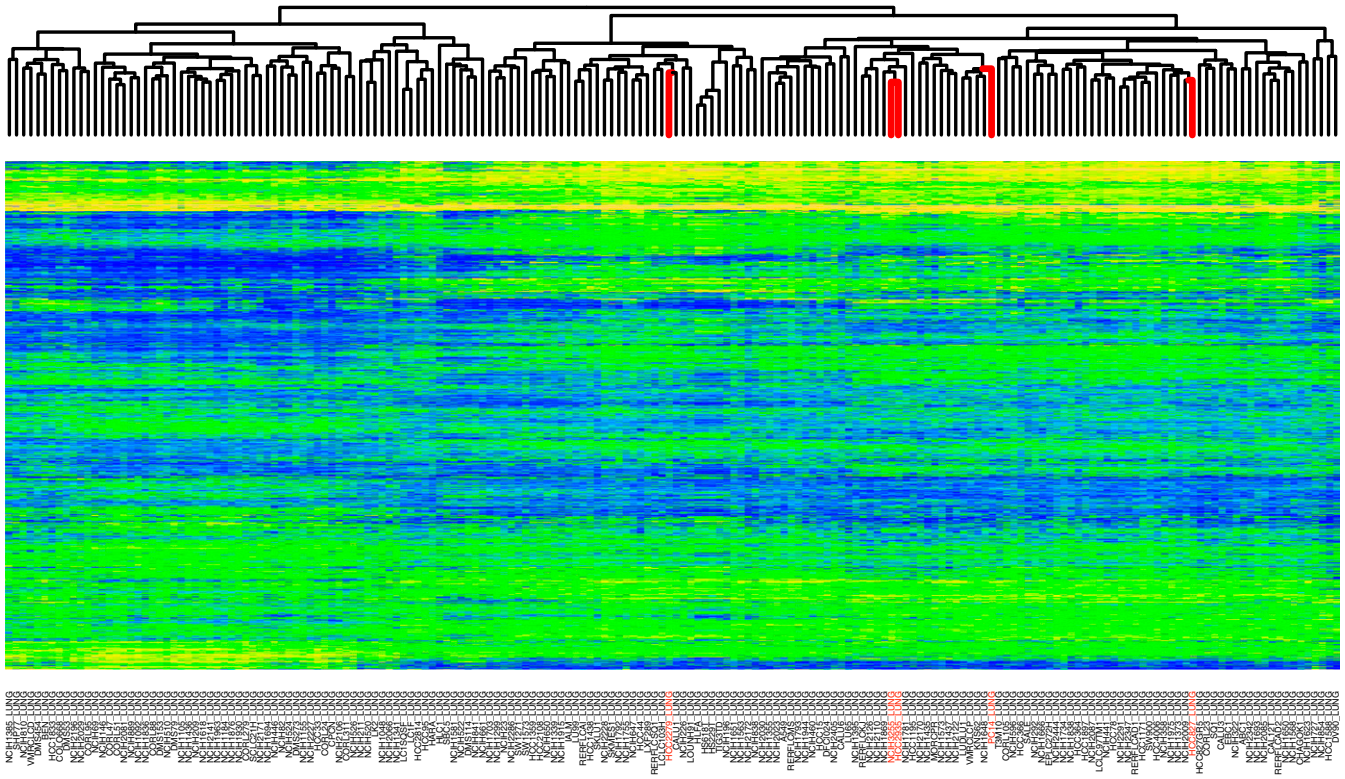

Fig. S3. *EGFR*-mutant cell lines are transcriptionally heterogeneous. The 186 NSCLC cell lines were clustered according to microarray gene expression profiles obtained as part of the Cancer Cell Line Encyclopedia (CCLE). Rows represent genes and columns represent cell lines. Heat map colors represent 8 $\log_2$ robust multiarray average (RMA) units of expression, ranging from blue (<6 $\log_2$ RMA units) to bright yellow (>12 $\log_2$ RMA units). The *EGFR*-mutant cell lines used for screening and/or validation studies are labeled red. The PC14 cell line has been reported to be misidentified and likely identical to PC9 by the CCLE's supplier of this line (Riken).

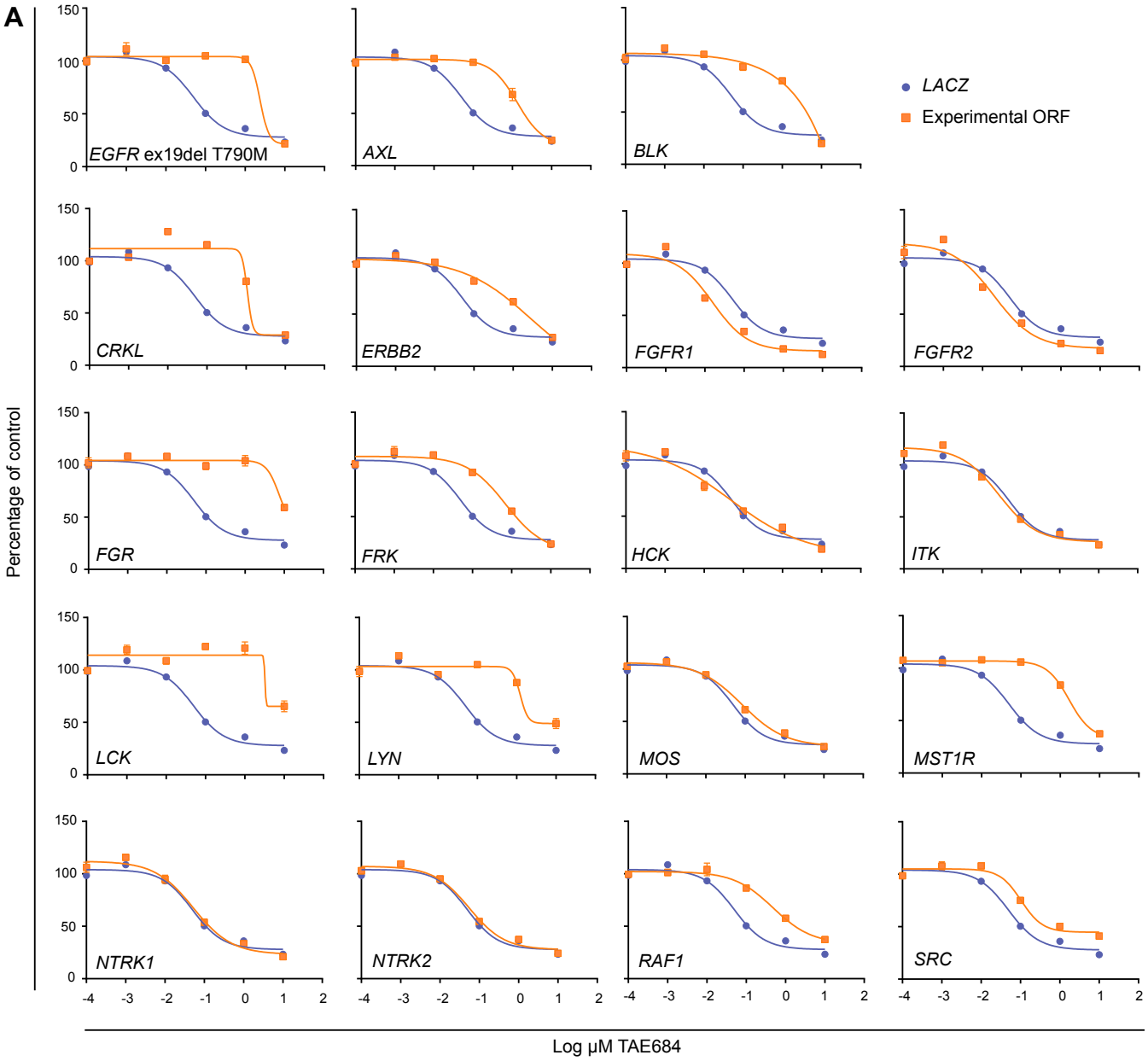

Fig. S4. (Continued)

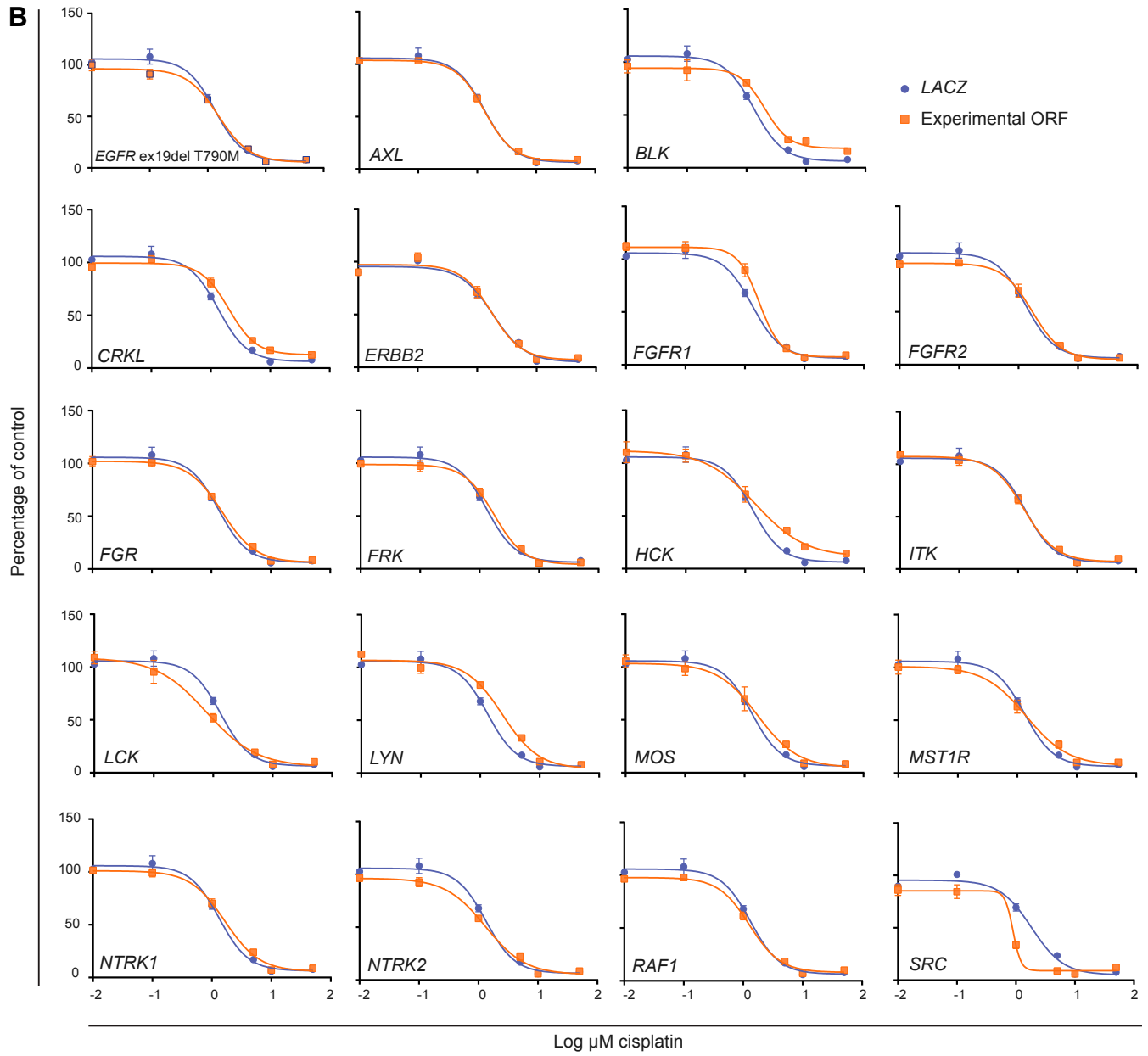

Fig. S4. A subset of EGFR bypass genes can promote resistance to ALK inhibition in ALK-dependent cells, but EGFR bypass genes fail to promote resistance to cisplatin in PC9 cells. (*A*) *EML4-ALK*-positive H3122 cells expressing EGFR bypass genes and controls were treated with indicated doses of TAE684 or vehicle, then assayed for cell viability after 72 h using CellTiter-Glo. Data are expressed as percent viability relative to vehicle-treated cells and represent the mean ± SD of four replicates. Graphs with identical control curves reflect experiments performed in parallel on the same day. (*B*) PC9 cells expressing EGFR bypass genes and controls were treated with indicated doses of cisplatin or vehicle, then assayed for cell viability after 72 h using CellTiter-Glo. Data are expressed as percent viability relative to vehicle-treated cells and represent the mean ± SD of four replicates. Graphs with identical control curves reflect experiments performed in parallel on the same day.

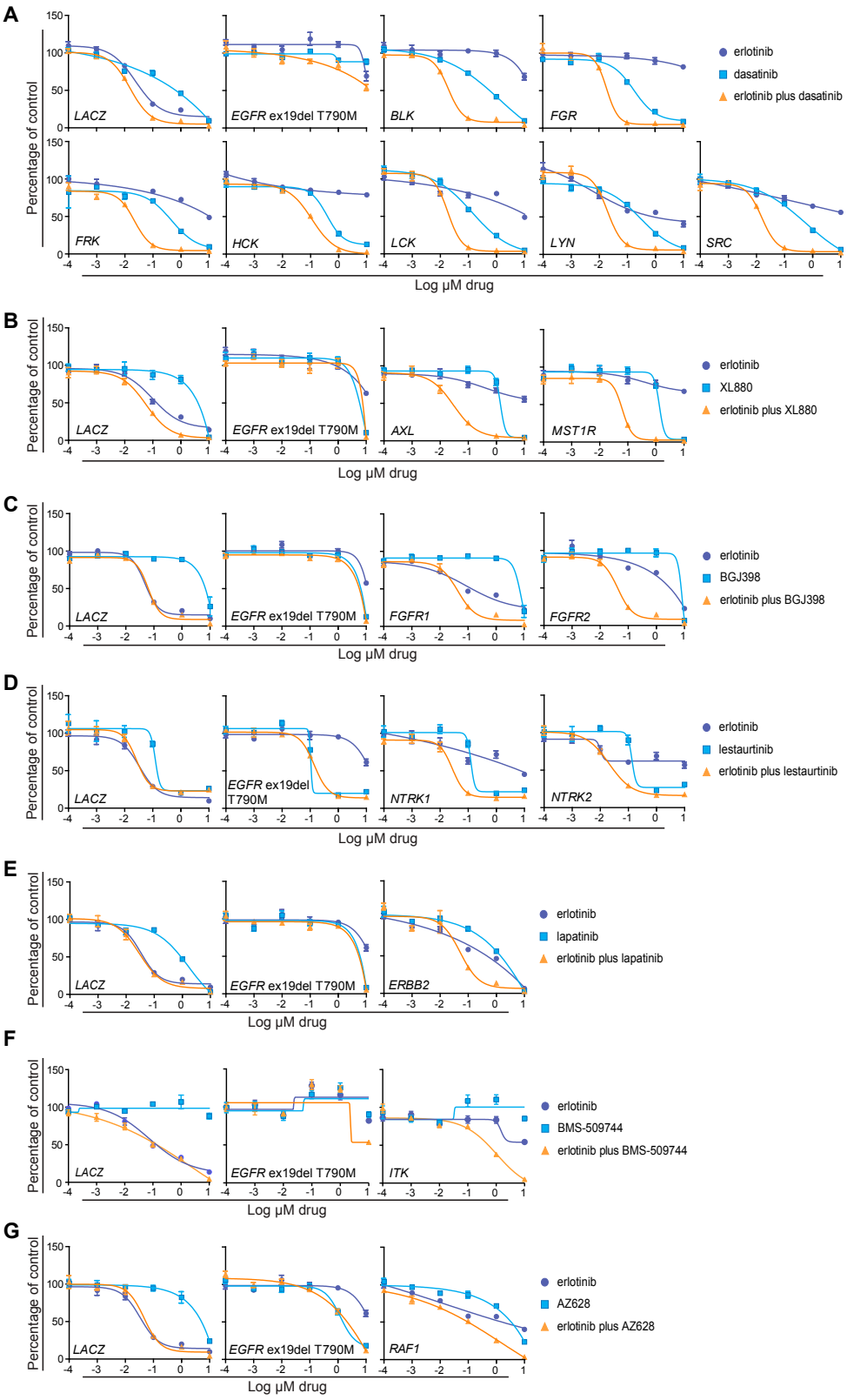

Fig. S5. (Continued)

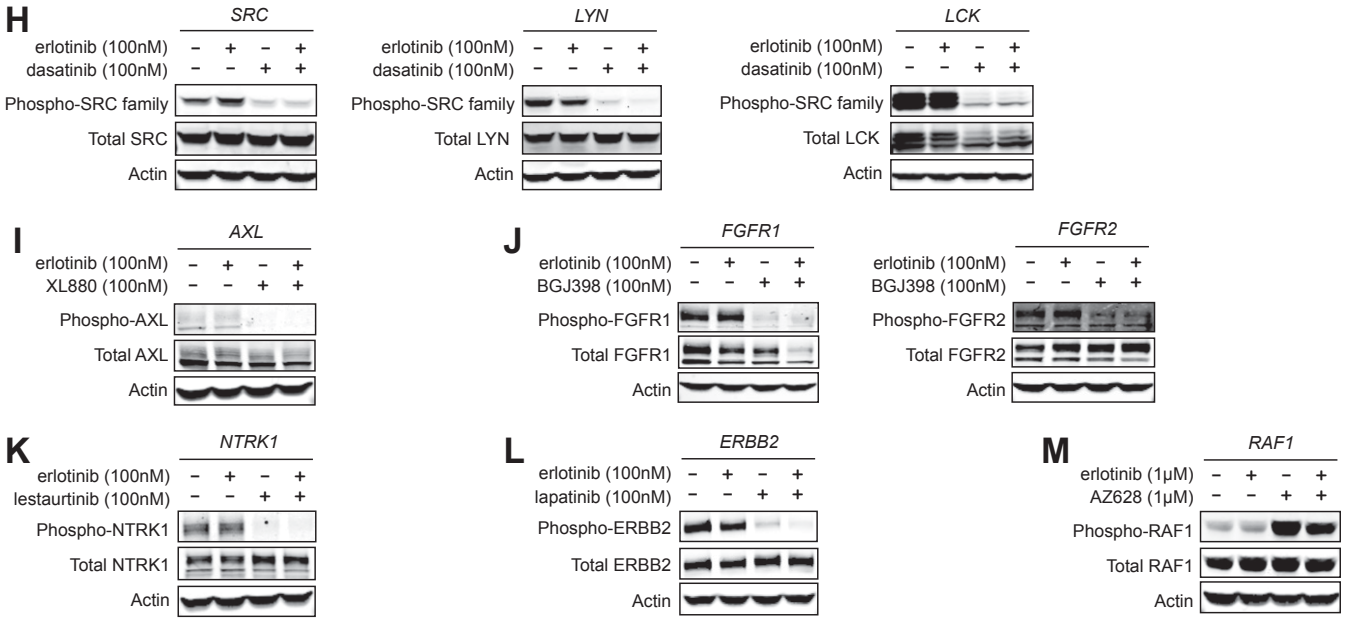

Fig. S5. Pharmacological blockade of EGFR bypass kinases restores sensitivity to erlotinib. Cell viability of PC9 cells overexpressing indicated EGFR bypass-inducing kinases and controls following treatment with increasing concentrations of erlotinib (purple curve), the relevant kinase inhibitor (light blue curve), or their combination (orange curve) for 72 h. Cell viability was assayed with CellTiter-Glo. Data are expressed as percent viability relative to vehicle-treated cells and represent the mean ± SD of ≥3 replicates. These dose–response curves were used to generate AUC values, plotted in Fig. 3*A*. Kinase inhibitors tested included (*A*) dasatinib for Src family kinases; (*B*) XL880 for AXL and MST1R; (*C*) BGJ398 for FGFR family kinases; (*D*) lestaurtinib for NTKR family kinases; (*E*) lapatinib for ERBB2; (*F*) BMS-509744 for ITK; and (*G*) AZ628 for RAF1. Graphs with identical control curves reflect experiments performed in parallel on the same day. (*H–M*) Immunoblot analysis of PC9 cells expressing EGFR bypass kinases under combination drug treatment. Transduced cells were treated with indicated doses of erlotinib, the relevant kinase inhibitor, or a combination for 6 h. Cells were incubated with 0.5% serum media 18 h before and during drug/DMSO treatment. Total cell lysates were immunoblotted for the indicated proteins. Kinase inhibitors tested included (*H*) dasatinib for Src family kinases SRC, LYN, and LCK; (*I*) XL880 for AXL; (*J*) BGJ398 for FGFR family kinases FGFR1 and FGFR2; (*K*) lestaurtinib for NTRK1; (*L*) lapatinib for ERBB2; and (*M*) AZ628 for RAF1. Except for with AZ628 (see main text), treatment with the relevant kinase inhibitors reduces phosphorylation of the target kinases tested.

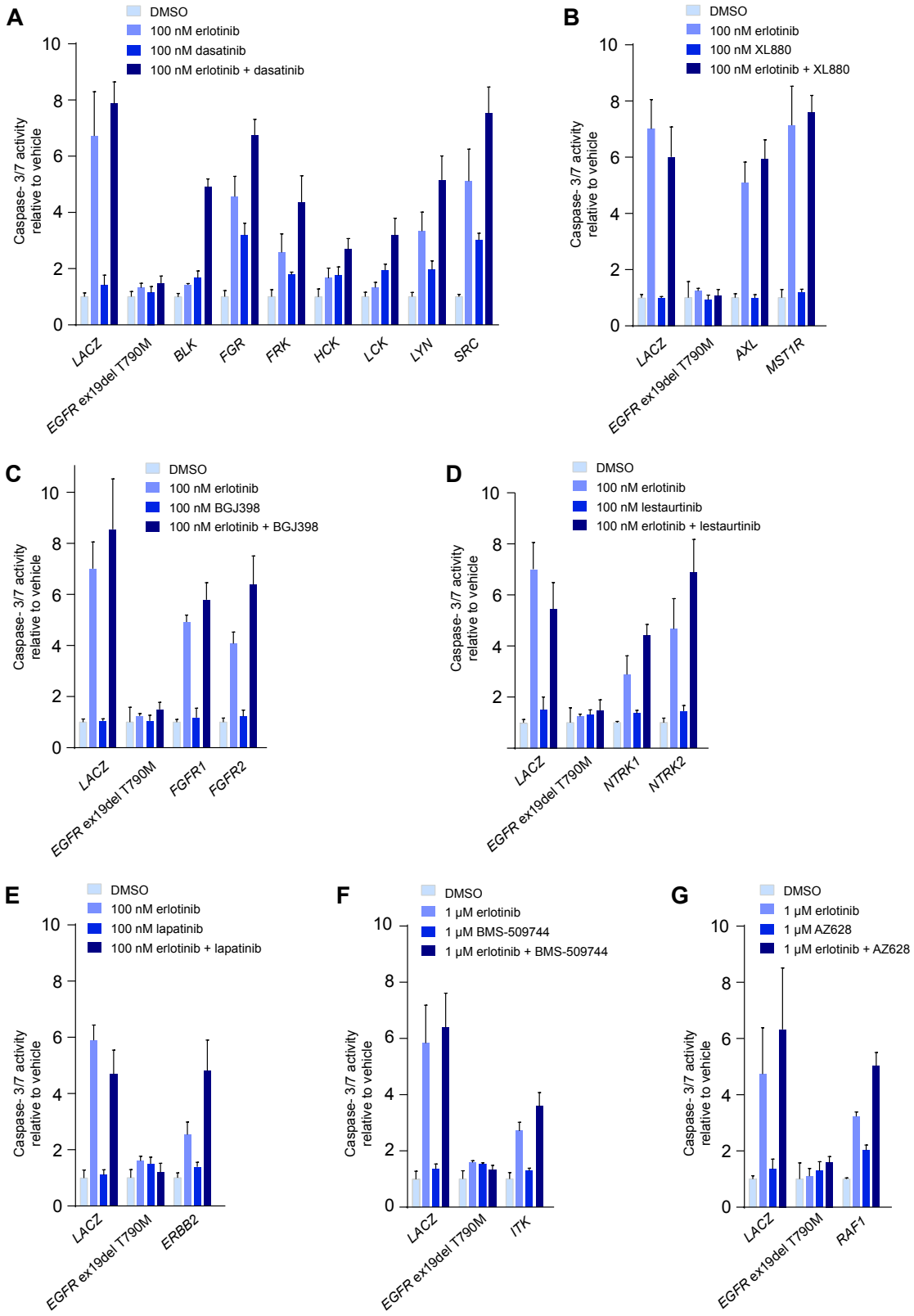

Fig. S6. Inhibition of EGFR bypass kinases enhances erlotinib-induced apoptosis. Caspase-3/7 activity of PC9 cells overexpressing indicated EGFR bypass-inducing kinases and controls following treatment with erlotinib, the relevant kinase inhibitor, or their combination for 26 h. Caspase-3/7 activity was measured with Caspase-Glo. Data are expressed as caspase-3/7 activity relative to vehicle-treated cells and represent the mean ± SD of four replicates. Kinase inhibitors tested included (*A*) dasatinib for Src family kinases; (*B*) XL880 for AXL and MST1R; (*C*) BGJ398 for FGFR family kinases; (*D*) lestaurtinib for NTKR family kinases; (*E*) lapatinib for ERBB2; (*F*) BMS-509744 for ITK; and (*G*) AZ628 for RAF1. Graphs with identical control values reflect experiments performed in parallel on the same day.

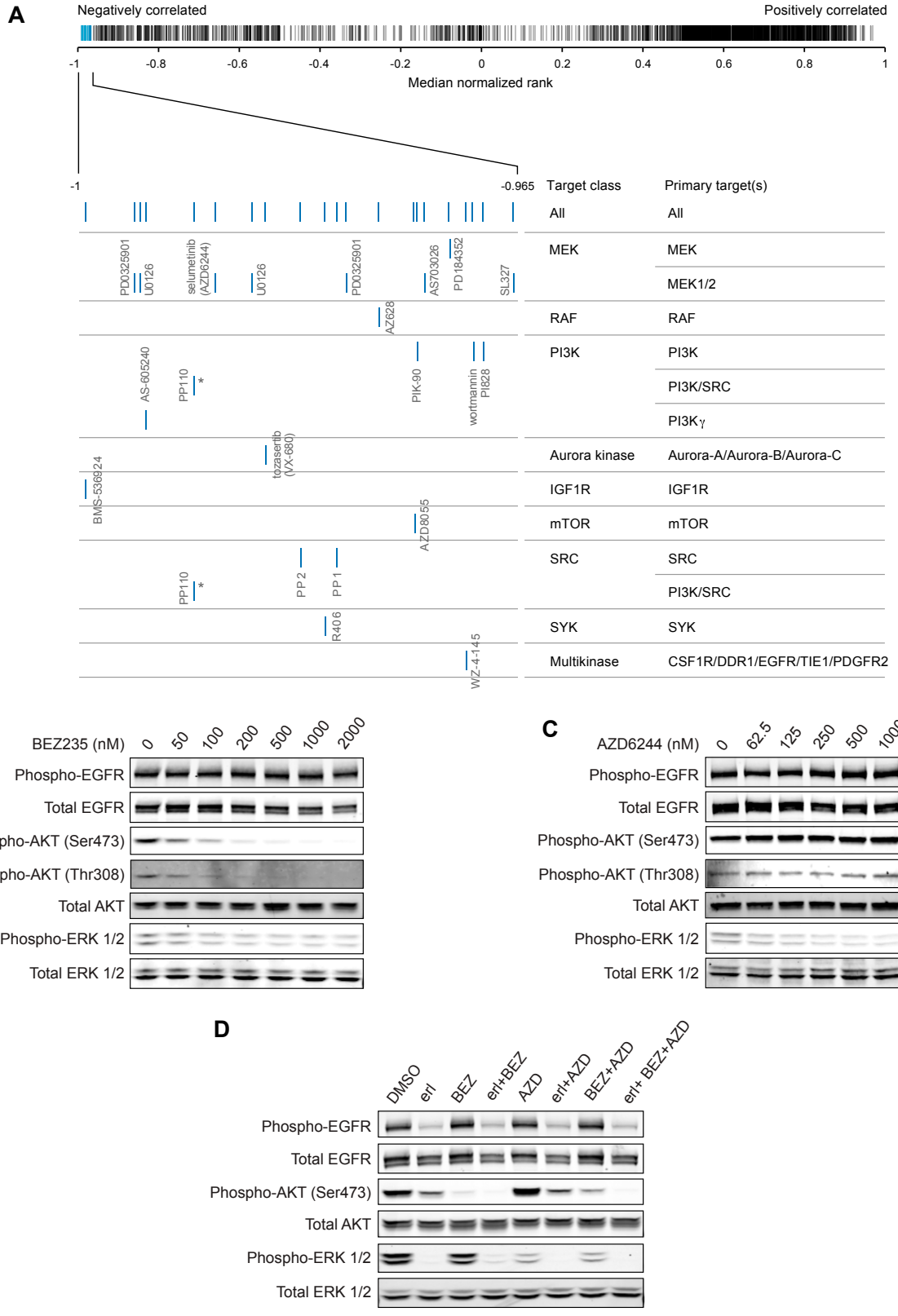

Fig. S7. LINCS compounds whose transcriptional effects most negatively correlate with those of EGFR bypass-mediating ORFs. (*A*) Median normalized ranks of the top 0.7% negatively correlated compounds and categorization by drug target class and primary target(s) (1–17). Each bar represents a compound. A single compound targeting both PI3K and SRC is denoted with an asterisk. (*B–D*) BEZ235 and AZD6244 treatment down-regulate phospho-AKT and phospho-ERK1/2, respectively, in a dose-dependent fashion. (*B*) Immunoblot analysis of PC9 cells treated with indicated doses of the PI3K-mTOR inhibitor BEZ235 for 6 h. Total cell lysates were immunoblotted for the indicated proteins. (*C*) Immunoblot analysis of PC9 cells treated with indicated doses of the MEK inhibitor AZD6244 for

Legend continued on following page

4 h. Total cell lysates were immunoblotted for the indicated proteins. (*D*) Immunoblot analysis of PC9 cells treated with 100 nM erlotinib (erl), 500 nM BEZ235 (BEZ), 2.5 μM AZD6244 (AZD), or their combinations for 6 h. Total cell lysates were immunoblotted for the indicated proteins.

1. Wittman M, et al. (2005) Discovery of a (1H-benzoimidazol-2-yl)-1H-pyridin-2-one (BMS-536924) inhibitor of insulin-like growth factor I receptor kinase with in vivo antitumor activity. *J Med Chem* 48(18):5639–5643.
2. Frémin C, Meloche S (2010) From basic research to clinical development of MEK1/2 inhibitors for cancer therapy. *J Hematol Oncol* 3:8.
3. Favata MF, et al. (1998) Identification of a novel inhibitor of mitogen-activated protein kinase kinase. *J Biol Chem* 273(29):18623–18632.
4. Camps M, et al. (2005) Blockade of PI3Kgamma suppresses joint inflammation and damage in mouse models of rheumatoid arthritis. *Nat Med* 11(9):936–943.
5. Apsel B, et al. (2008) Targeted polypharmacology: Discovery of dual inhibitors of tyrosine and phosphoinositide kinases. *Nat Chem Biol* 4(11):691–699.
6. Yeh TC, et al. (2007) Biological characterization of ARRY-142886 (AZD6244), a potent, highly selective mitogen-activated protein kinase kinase 1/2 inhibitor. *Clin Cancer Res* 13(5): 1576–1583.
7. Harrington EA, et al. (2004) VX-680, a potent and selective small-molecule inhibitor of the Aurora kinases, suppresses tumor growth in vivo. *Nat Med* 10(3):262–267.
8. Hanke JH, et al. (1996) Discovery of a novel, potent, and Src family-selective tyrosine kinase inhibitor. Study of Lck- and FynT-dependent T cell activation. *J Biol Chem* 271(2):695–701.
9. Khazak V, Astsaturov I, Serebriiskii IG, Golemis EA (2007) Selective Raf inhibition in cancer therapy. *Expert Opin Ther Targets* 11(12):1587–1609.
10. Chresta CM, et al. (2010) AZD8055 is a potent, selective, and orally bioavailable ATP-competitive mammalian target of rapamycin kinase inhibitor with in vitro and in vivo antitumor activity. *Cancer Res* 70(1):288–298.
11. Knight ZA, et al. (2006) A pharmacological map of the PI3-K family defines a role for p110alpha in insulin signaling. *Cell* 125(4):733–747.
12. Kim K, et al. (2010) Blockade of the MEK/ERK signalling cascade by AS703026, a novel selective MEK1/2 inhibitor, induces pleiotropic anti-myeloma activity in vitro and in vivo. *Br J Haematol* 149(4):537–549.
13. Sebolt-Leopold JS, et al. (1999) Blockade of the MAP kinase pathway suppresses growth of colon tumors in vivo. *Nat Med* 5(7):810–816.
14. Kim HG, et al. (2013) Discovery of a potent and selective DDR1 receptor tyrosine kinase inhibitor. *ACS Chem Biol* 8(10):2145–2150.
15. Yano H, et al. (1993) Inhibition of histamine secretion by wortmannin through the blockade of phosphatidylinositol 3-kinase in RBL-2H3 cells. *J Biol Chem* 268(34):25846–25856.
16. Gharbi SI, et al. (2007) Exploring the specificity of the PI3K family inhibitor LY294002. *Biochem J* 404(1):15–21.
17. Scherle PA, Ma W, Lim H, Dey SK, Trzaskos JM (2000) Regulation of cyclooxygenase-2 induction in the mouse uterus during decidualization. An event of early pregnancy. *J Biol Chem* 275(47):37086–37092.

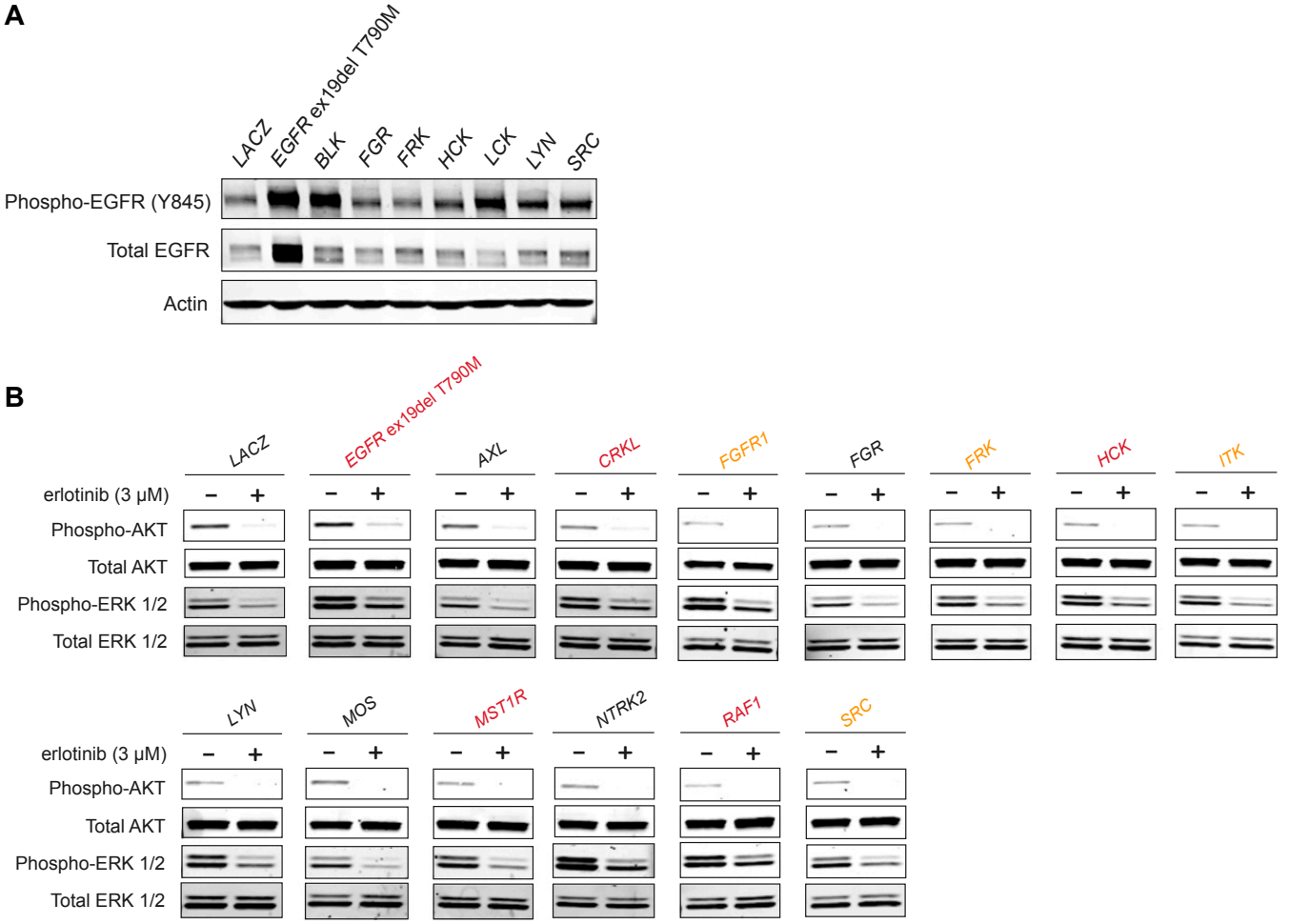

Fig. S8. ORF-induced signaling activation in PC9 and H3255 cells. (*A*) Overexpression of Src family kinases leads to phosphorylation of tyrosine 845 on EGFR. Immunoblot analysis of PC9 cells overexpressing Src family kinases and control ORFs following treatment with DMSO for 6 h. Cells were incubated with 0.5% serum media 18 h before and during DMSO treatment. (*B*) Resistance-promoting genes frequently reactivate ERK1/2 signaling in H3255 cells. Immunoblot analysis of H3255 cells overexpressing the indicated ORFs and treated with erlotinib for 6 h. Cells were incubated with 0.5% serum media 18 h before and during drug/DMSO treatment. Colors denote significance and effect size of a given ORF's resistance-promoting effect in H3255 cells, relative to *LACZ*, as determined from Fig. S2. Black, not significant; orange, significant with fold-change ≤1.20; red, significant with fold-change >1.20.

Table S1. IC_{50} values of ORF-screen validation experiments in PC9 cells

	Validation experiment IC_{50} value, μM				
Gene	*LACZ*	*LUCIFERASE*	*EGFR*-L858R-T790M	*EGFR*-ex19del-T790M	Experimental ORF
AXL	0.042	0.046	>10	>10	>10
BLK	0.022	0.023	8.7	8.4	>10
CRKL	0.022	0.023	8.7	8.4	>10
ERBB2	0.022	0.023	8.7	8.4	0.79
FGR	0.022	0.023	8.7	8.4	3.6
FGFR1	0.042	0.046	>10	>10	0.19
FGFR2	0.057	0.082	>10	>10	1.2
FRK	0.022	0.023	8.7	8.4	0.29
HCK	0.022	0.023	8.7	8.4	>10
ITK	0.022	0.023	8.7	8.4	1.4
LCK	0.022	0.023	8.7	8.4	0.34
LYN	0.022	0.023	8.7	8.4	0.054
MOS	0.042	0.046	>10	>10	2.3
MST1R	0.022	0.023	8.7	8.4	0.53
NTRK1	0.022	0.023	8.7	8.4	0.41
NTRK2	0.022	0.023	8.7	8.4	0.11
RAF1	0.022	0.023	8.7	8.4	6.2
SRC	0.022	0.023	8.7	8.4	1.7
YES1	0.022	0.023	8.7	8.4	0.031

Absolute IC_{50} values correspond to validation experiments described in Fig. 2*A*.